Journal of Pathology
J Pathol March 2022; **256:** 256–261
Published online 10 January 2022 in Wiley Online Library (wileyonlinelibrary.com) DOI: 10.1002/path.5842

BRIEF REPORT

Indoleamine 2,3-dioxygenase (IDO)-1 and IDO-2 activity and severe course of COVID-19

Lihui Guo[1], Bernadette Schurink[2], Eva Roos[2], Esther J Nossent[3], Jan Willem Duitman[3], Alexander PJ Vlaar[4], Paul van der Valk[2], Frédéric M Vaz[5], Syun-Ru Yeh[6], Zachary Geeraerts[6], Annemiek Dijkhuis[1], Lonneke van Vught[4], Marianna Bugiani[2], and René Lutter,[1,3]*
also on behalf of the Amsterdam UMC COVID-19 Biobank Study Group†

[1] *Department of Experimental Immunology, Amsterdam University Medical Centers (UMC) and Amsterdam Infection and Immunity Institute, University of Amsterdam, Amsterdam, The Netherlands*
[2] *Department of Pathology, Amsterdam UMC, VU University Amsterdam, Amsterdam, The Netherlands*
[3] *Department of Respiratory Medicine, Amsterdam UMC, University of Amsterdam and VU University Amsterdam, Amsterdam, The Netherlands*
[4] *Department of Intensive Care and Center for Experimental Molecular Medicine, Amsterdam UMC, University of Amsterdam, Amsterdam, The Netherlands*
[5] *Laboratory Genetic Metabolic Diseases, Core Facility Metabolomics, Department of Clinical Chemistry, Amsterdam University Medical Center, University of Amsterdam, Amsterdam, The Netherlands*
[6] *Department of Physiology and Biophysics, Albert Einstein College of Medicine, Bronx, NY, USA*

**Correspondence to: René Lutter, Department of Respiratory Medicine, Amsterdam UMC, Location AMC, Room F5-152, Meibergdreef 9, 1105 AZ Amsterdam, The Netherlands. E-mail: r.lutter@amsterdamumc.nl*

†See supplementary material, Table S1 for a full list of participants.

Abstract

COVID-19 is a pandemic with high morbidity and mortality. In an autopsy cohort of COVID-19 patients, we found extensive accumulation of the tryptophan degradation products 3-hydroxy-anthranilic acid and quinolinic acid in the lungs, heart, and brain. This was not related to the expression of the tryptophan-catabolizing indoleamine 2,3-dioxygenase (IDO)-1, but rather to that of its isoform IDO-2, which otherwise is expressed rarely. Bioavailability of tryptophan is an absolute requirement for proper cell functioning and synthesis of hormones, whereas its degradation products can cause cell death. Markers of apoptosis and severe cellular stress were associated with IDO-2 expression in large areas of lung and heart tissue, whereas affected areas in brain were more restricted. Analyses of tissue, cerebrospinal fluid, and sequential plasma samples indicate early initiation of the kynurenine/aryl-hydrocarbon receptor/IDO-2 axis as a positive feedback loop, potentially leading to severe COVID-19 pathology.

Keywords: tryptophan; apoptosis; autophagy; innate_immune_response; lungs; brain; heart; skeletal_muscle; nucleus_of_cranial_nerve_X

Received 17 May 2021; Revised 12 November 2021; Accepted 30 November 2021

No conflicts of interest were declared.

Introduction

The clinical course of severe acute respiratory syndrome coronavirus 2 (SARS-CoV-2) infections varies greatly, from asymptomatic to fatal coronavirus disease 2019 (COVID-19) [1].

Many studies indicate an important role of the immune system in COVID-19, with the tryptophan–kynurenine pathway as a possible important immune-modulator affecting the course of disease [2,3]. The immune-modulating capacity of the tryptophan–kynurenine pathway is facilitated both by depletion of tryptophan, halting cell activation, and by inducing cell death via cytotoxic kynurenine and downstream catabolites [4]. Indoleamine 2,3-dioxygenase-1 (IDO-1) and its isoform IDO-2 are inducible and rate-limiting enzymes oxidizing tryptophan to *N*-formyl-kynurenine, which is degraded further by cytoplasmic enzymes. Typically, IDO-1 is induced by interferons during viral infections and can persist for several weeks after viral clearance [5,6]. IDO-2 is expressed rarely [7] and is induced by the aryl hydrocarbon receptor (AHR), but not by interferons [8,9].

Recently, we performed whole body autopsies on 21 patients who died with COVID-19, who were hospitalized from 5 days to 6 weeks, 41–78 (median 68) years of age, and 76% of whom had comorbidities [10]. Besides the lungs, other organs including the brain were also inflamed but to variable extents. A key pathological finding, particularly in patients with long-lasting COVID-19, was the relatively low number of viral

particles. This led us to hypothesize that severe COVID-19 pathology is due to a systemic autonomous process [11]. Here, we report on the IDO–kynurenine pathway in severe COVID-19. As limited bioavailability of tryptophan results in autophagy [12,13], and cytotoxic metabolites from the kynurenine pathway induce apoptosis [14,15], we also assessed markers of these processes.

Materials and methods

Study set-up

The design of the prospective autopsy cohort study and relevant procedures have been provided previously [10]. Demographics are provided in supplementary material, Table S2. Cerebrospinal fluid (CSF) samples from patients with or without COVID-19 were collected within 24 h post-mortem, taken from lateral ventricles, not centrifuged, and stored at −80 °C. Ethical approval was granted by the institutional review board of Amsterdam UMC (2020.167) and informed consent was obtained.

Immunohistochemistry

Immunohistochemical analyses of tissues from severe COVID-19 patients were performed as described previously [10]. Supplementary material, Table S3 provides an overview of the antibodies applied. Validation of IDO-2 staining is described in Supplementary materials and methods and supplementary materials, Figure S1.

Quantitation of tryptophan, kynurenine, and metabolites

A mix of stable isotope-labeled internal standards was added to 50 µl of plasma or CSF. Samples were deproteinized using acetonitrile, dried under nitrogen, and reconstituted in 100 µl of 0.1% heptafluorobutyric acid. Aliquots (10 µl) of extracts were injected into a UPLC–MS/MS system comprising an Acquity Xevo TQ-XS system (Waters, Milford, MA, USA) operated in positive ESI mode using multiple reaction monitoring (MRM) for preselected analytes and an overall run time of 6 min. Additional details are provided in Supplementary materials and methods.

Results and discussion

Expression of IDO-1, IDO-2, and 3-hydroxy-anthranilic acid (3OH-AA) and quinolinic acid (QUIN), two major catabolic products of the tryptophan–kynurenine pathway, was determined immunohistochemically first in lung tissue from patients from the above-mentioned cohort. 3OH-AA and QUIN were expressed abundantly in the cytoplasm (Figure 1A–F). IDO-1 expression (Figure 1A–C) was sparse and mostly restricted to endothelial cells. IDO-2 expression, however, was abundant (Figure 1D–F) in the cytoplasm of, among others, interstitial cells, endothelial cells, and type 1 and type 2 pneumocytes. Both 3OH-AA and QUIN co-stained with IDO-1, but particularly with IDO-2, indicating that most of the IDO activity was due to IDO-2. Sections from patients who died on the day of ICU admission also stained for IDO-2 (supplementary material, Table S2). IDO-2 and 3OH-AA staining was virtually absent in lung tissue from patients with fatal heart infarct or bronchopneumonia (supplementary material, Figure S2).

Next, we assessed autophagy (LC3B) and apoptosis (cleaved caspase-3) as key indicators of severe metabolic stress relative to IDO-2 expression. Ki-67, indicative of proliferating cells, often co-exists with autophagy [16,17]. Cells in lung tissue expressing IDO-2 co-stained for cleaved caspase-3, LC3B, and Ki-67 (Figure 1G–L).

To determine whether IDO-2 expression was also manifest in other organs, we assessed the expression of IDO-2, LC3B, Ki-67, and cleaved caspase-3 in the heart, liver, and skeletal muscle. Skeletal muscle was expected to be the least affected tissue, as COVID-19-related myopathy is exceedingly rare. The heart and liver, like the lung, are inflamed in COVID-19, in which the liver was less likely to be affected by kynurenine and its metabolites because tryptophan dioxygenase in the liver regulates systemic tryptophan levels by generating *N*-formyl-kynurenine. Compared with expression in the lung, IDO-2 expression was consecutively lower in the heart, skeletal muscle, and liver (supplementary material, Figure S3A–I). The latter two showed very little IDO-2 expression, apart from the skeletal muscle of one out of around 40 patients studied so far, who developed myositis with marked IDO-2 expression between degenerated muscle fibers. LC3B and Ki-67 co-localized with IDO-2, being less prominent in the heart compared with the lung and virtually absent in muscle and liver. Cleaved caspase-3 co-localized with IDO-2 also in the heart and was almost absent in the liver and muscle, apart from endothelial cells in various organs (supplementary material, Figure S3M–R). Taken together, these data show that IDO-2, LC3B, Ki-67, and cleaved caspase-3 are co-expressed mostly in the lungs, less in the heart, and negligibly in the liver and skeletal muscle. We next assessed whether IDO-2 expression was found also in migratory cells in addition to structural cells. Macrophages, dendritic cells, and neutrophils showed IDO-2 staining, but lymphocytes and mast cells did not (supplementary material, Figure S4).

Such high IDO-2 expression and activity are unprecedented. IDO-2 is induced by activation of the aryl hydrocarbon receptor (AHR), which can be triggered by kynurenine [8,9]. AHR expression in COVID-19 lung tissue co-localized with IDO-2 expression and was predominantly found in nuclei, indicative of transcriptionally active AHR (Figure 2A–C). A plausible explanation for IDO-2 expression in severe COVID-19 is therefore that IDO-1-generated kynurenine triggered IDO-2 expression and activity, resulting in a positive feedback loop (Figure 2I).

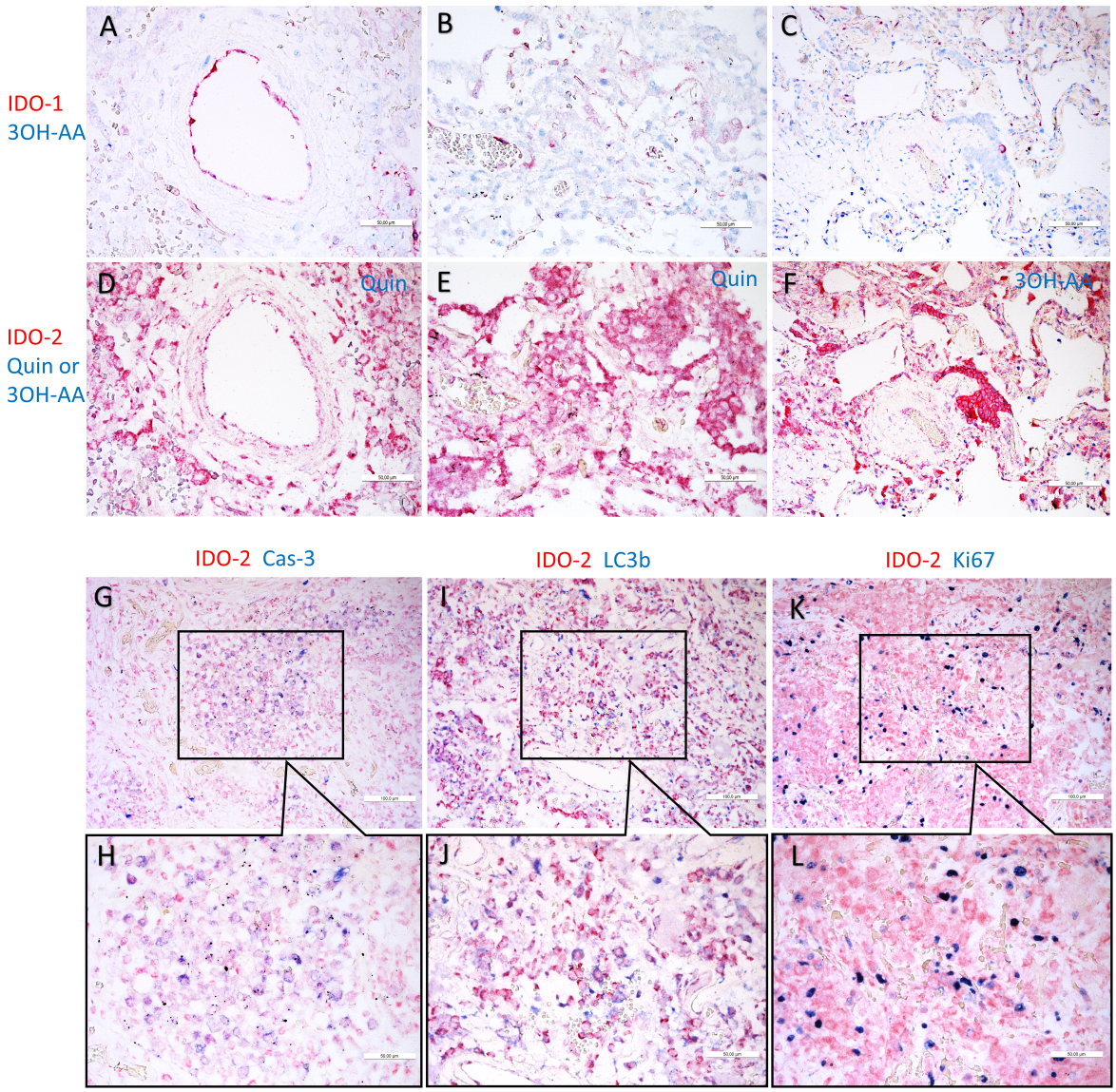

Figure 1. Tryptophan catabolism and cellular stress in lung tissue from patients who died with COVID-19. (A–F) Autopsy lung tissue sections stained for IDO-1, IDO-2, and kynurenine metabolites 3-hydroxy-anthranilic acid (3OH-AA) and quinolinic acid (QUIN). Representative images of lung tissue from five patients with COVID-19. (G–L) Autopsy lung tissue sections stained for IDO-2 and LC3B (marker of autophagy), Ki-67 (marker of cell proliferation), and cleaved caspase-3 (marker of apoptosis). Representative images of lung tissue from five patients with COVID-19. Magnifications are indicated in the lower right corner.

We reasoned that ependymal cells in the brain, which line the ventricular system and face the CSF, may be a primary site for exposure to systemic kynurenine. In line with this hypothesis, ependymal cells of the lateral ventricles were strongly IDO-2-positive and also stained for 3OH-AA (Figure 2D–F). There was a faint positivity for AHR in ependymal cells which was slightly more marked in the subventricular zone (Figure 2G,H). Whereas Ki-67, LC3B, and caspase-3 were found in association with IDO-2 expression in brain tissue (supplementary material, Figure S3J–L), we found no IDO-1 expression. In contrast to the lung and heart, IDO-2 expression in the investigated brain structures was not as extensive. Interestingly, many neurogenic astrocytes in the subventricular zone were apoptotic, which is indicative of a profound metabolic stress that may have major pathophysiological consequences. We also investigated the brainstem, where body regulatory functions are controlled. The dopaminergic nuclei in the nucleus of the tenth cranial nerve were intensely IDO-2-positive, as were the nuclei in the nucleus arcuatus (which connects cortico-spinal tracts to the cerebellum; supplementary material, Figure S5A,B). Many IDO-2-positive cells in nucleus X expressed nuclear AHR, were not apoptotic, but showed autophagy, like the surrounding cells (supplementary material, Figure S5A,D,E). In contrast, other brainstem nuclei including the serotoninergic neurons in the raphe, which are involved in tryptophan metabolism, were only slightly IDO-2-positive (supplementary material, Figure S5C).

To clarify whether tissue IDO-2 activity was detectable systemically, we assessed tryptophan, kynurenine,

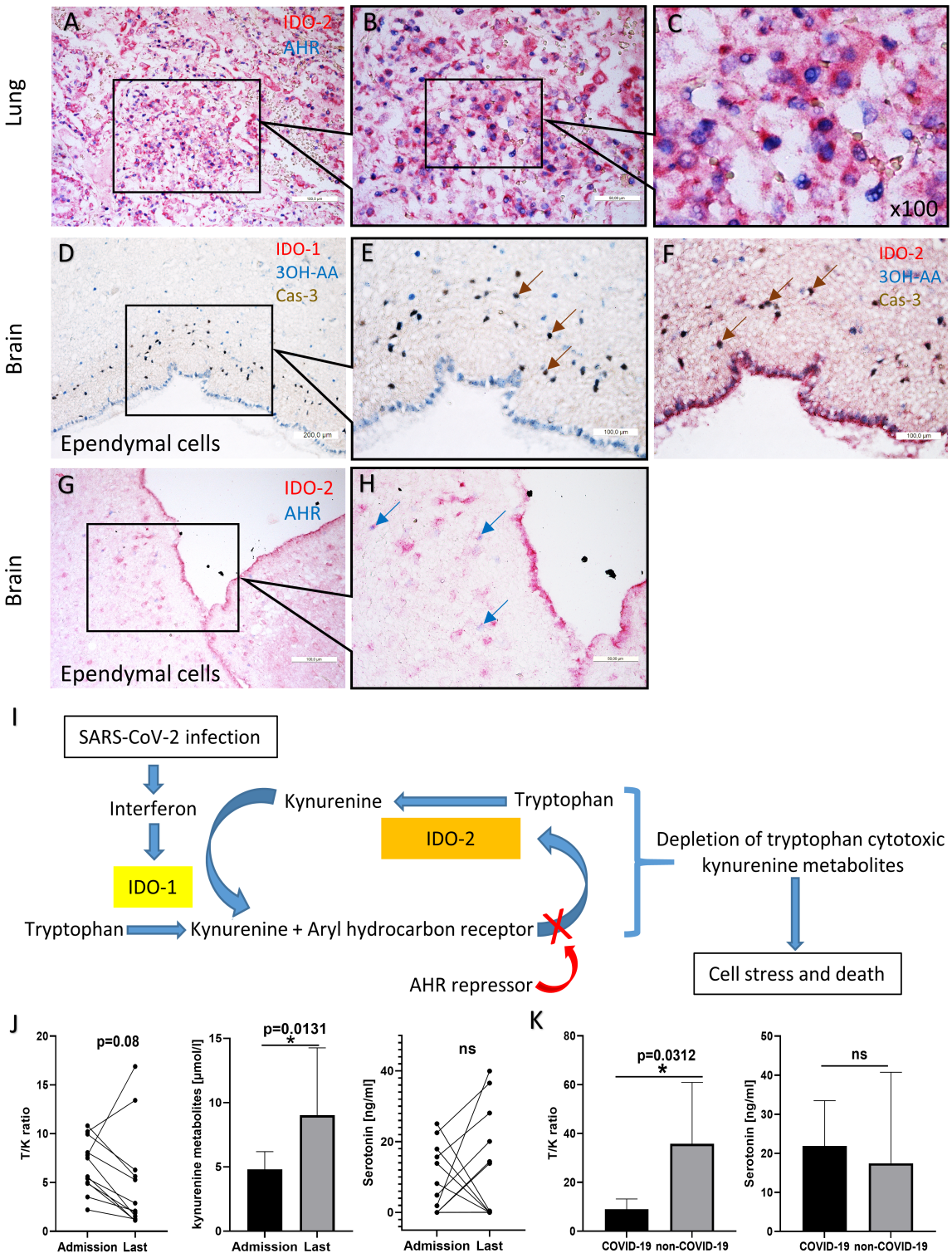

Figure 2. The aryl hydrocarbon receptor and systemic kynurenine in patients who died with COVID-19. (A–H) IDO-2 and AHR expression in ependymal cells and lung. Representative images of tissues from three patients with COVID-19. (I) Schematic representation of the kynurenine–aryl hydrocarbon receptor axis. (J, K) Tryptophan/kynurenine ratio, kynurenine metabolites, and serotonin in plasma and CSF. Plasma from 12 patients; CSF from ten patients with COVID-19 and six without COVID-19. Colored arrows indicate staining of the marker represented by the color.

and downstream metabolites in EDTA-plasma collected from patients just after admission to the intensive care unit, in intermediate samples when available, and shortly before death of patients with COVID-19. The interval between the latter sampling and death varied from 0 to 4 days (with the following distribution: median 0 days, interquartile range 0–2 days). Tryptophan concentrations in plasma at admission and in the last sample before death were 30.1 ± 10 and 25.5 ± 9.4 µmol/l (mean ± SD), respectively. The tryptophan/kynurenine (T/K) ratio

declined in most patients, apart from two (Figure 2J). As patients were nourished with proteins and/or amino acids, this may have led to biased T/K ratios. Therefore, we also analyzed the sum of only kynurenine and downstream metabolites in plasma, which increased significantly over time. Tryptophan concentrations in CSF from patients with and without COVID-19 were 24.8 ± 18.9 and 19.4 ± 16.4 μmol/l (mean ± SD), respectively. The presence of tryptophan degradation products was confirmed in CSF from patients with COVID-19, compared with patients without COVID-19 (Figure 2K). As tryptophan is required for serotonin synthesis, we also measured serotonin in EDTA-plasma and CSF (Figure 2J,K). Despite a decreased T/K ratio in CSF, we found no reduced levels of serotonin in CSF. This finding is in line with the low level of IDO-2 expression in the serotoninergic brainstem raphe neurons. In plasma, we found both increased and reduced serotonin levels over time, where increased levels corresponded with deep vein thrombosis and/or pulmonary embolism, suggestive of serotonin released by thrombocytes.

Our findings support systemic and early activation of IDO-2 expression and activity via AHR in severe COVID-19, resulting in severe cellular stress reflected by autophagy and apoptosis, particularly in the lungs, heart, brain, and endothelium. As some innate immune cells also express IDO-2, it is likely that immune responses are attenuated in severe COVID-19. Although we did not find similar stains in control lung tissue or that of patients with fatal bronchopneumonia, we cannot exclude the possibility that similar findings may be obtained in, for example, fatal influenza. The involvement of AHR is in line with a recent study reporting reduced mRNA expression of aryl hydrocarbon receptor repressor (*AHRR*) in the lungs from patients with fatal COVID-19 with a relatively low viral load [18]. Similarly, in obese individuals with a higher risk factor for severe COVID-19, reduced levels of AHRR were found [19,20]. IDO-2 and AHR are possible targets to prevent severe COVID-19-related pathology.

Acknowledgements

We acknowledge the assistance of the mortuary staff of the Expert Center for Post-mortem Diagnostics of the Amsterdam UMC. We thank Professor Benoit van den Eynde (Ludwig Institute for Cancer Research, Université Catholique de Louvain, Brussels, Belgium) for providing anti-IDO-1. Professor Harm Jan Bogaard and Dr Daniel Koorevaar (Department of Respiratory Medicine, Amsterdam UMC, location VUMC) are acknowledged for discussions.

Author contributions statement

LG contributed to the design of the study, performed and interpreted stains, and drafted the manuscript. BS, ER, PvdV, and MB contributed to the design of the study, provided tissue samples, performed and interpreted stains, and contributed to the draft manuscript. EJN, JWD, and APJV contributed to the design of the study and to the draft manuscript. FV analyzed metabolites and contributed to the draft manuscript. S-RY and ZG provided recombinant human IDO-2 and advised on its use. AD performed analyses to show specificity of the IDO-2 antibody and performed the PCR analyses. LvV helped with sample selection and contributed to the draft manuscript. RL designed the study, interpreted results, and drafted the manuscript. The Amsterdam UMC COVID-19 Biobank Study Group (supplementary material, Table S1) was responsible for the clinical care of COVID-19 patients and helped to collect, provide, and select plasma samples. All the authors had full access to data and approved the final version of the manuscript.

References

1. Wiersinga WJ, Rhodes A, Cheng AC, *et al*. Pathophysiology, transmission, diagnosis, and treatment of coronavirus disease 2019 (COVID-19): a review. *JAMA* 2020; **324:** 782–793.
2. Thomas T, Stefanoni D, Reisz JA, *et al*. COVID-19 infection alters kynurenine and fatty acid metabolism, correlating with IL-6 levels and renal status. *JCI Insight* 2020; **5:** e140327.
3. Blasco H, Bessy C, Plantier L, *et al*. The specific metabolome profiling of patients infected by SARS-COV-2 supports the key role of tryptophan-nicotinamide pathway and cytosine metabolism. *Sci Rep* 2020; **10:** 16824.
4. Munn DH, Mellor AL. Indoleamine 2,3 dioxygenase and metabolic control of immune responses. *Trends Immunol* 2013; **34:** 137–143.
5. Fox JM, Crabtree JM, Sage LK, *et al*. Interferon lambda upregulates IDO1 expression in respiratory epithelial cells after influenza virus infection. *J Interferon Cytokine Res* 2015; **35:** 554–562.
6. van der Sluijs KF, Nijhuis M, Levels JH, *et al*. Influenza-induced expression of indoleamine 2,3-dioxygenase enhances interleukin-10 production and bacterial outgrowth during secondary pneumococcal pneumonia. *J Infect Dis* 2006; **193:** 214–222.
7. Ball HJ, Sanchez-Perez A, Weiser S, *et al*. Characterization of an indoleamine 2,3-dioxygenase-like protein found in humans and mice. *Gene* 2007; **396:** 203–213.
8. Li Q, Harden JL, Anderson CD, *et al*. Tolerogenic phenotype of IFN-γ-induced IDO^{+} dendritic cells is maintained via an autocrine IDO–kynurenine/AhR–IDO loop. *J Immunol* 2016; **197:** 962–970.
9. Fukunaga M, Yamamoto Y, Kawasoe M, *et al*. Studies on tissue and cellular distribution of indoleamine 2,3-dioxygenase 2: the absence of IDO1 upregulates IDO2 expression in the epididymis. *J Histochem Cytochem* 2012; **60:** 854–860.
10. Schurink B, Roos E, Radonic T, *et al*. Viral presence and immunopathology in patients with lethal COVID-19: a prospective autopsy cohort study. *Lancet Microbe* 2020; **1:** e290–e299.
11. Lutter R, Schurink B, Roos E, *et al*. Neutrophils as a pallbearer for SARS-CoV-2 disease burden – authors' reply. *Lancet Microbe* 2021; **2:** e57.
12. Munn DH, Sharma MD, Baban B, *et al*. GCN2 kinase in T cells mediates proliferative arrest and anergy induction in response to indoleamine 2,3-dioxygenase. *Immunity* 2005; **22:** 633–642.
13. Fougeray S, Mami I, Bertho G, *et al*. Tryptophan depletion and the kinase GCN2 mediate IFN-γ-induced autophagy. *J Immunol* 2012; **189:** 2954–2964.
14. Guillemin GJ, Wang L, Brew BJ. Quinolinic acid selectively induces apoptosis of human astrocytes: potential role in AIDS dementia complex. *J Neuroinflammation* 2005; **2:** 16.

15. Hiramatsu R, Hara T, Akimoto H, *et al*. Cinnabarinic acid generated from 3-hydroxyanthranilic acid strongly induces apoptosis in thymocytes through the generation of reactive oxygen species and the induction of caspase. *J Cell Biochem* 2008; **103:** 42–53.
16. Gorska-Ponikowska M, Kuban-Jankowska A, Daca A, *et al*. 2-Methoxyestradiol reverses the pro-carcinogenic effect of L-lactate in osteosarcoma 143B cells. *Cancer Genomics Proteomics* 2017; **14:** 483–493.
17. Oikonomou P, Giatromanolaki A, Tsaroucha AK, *et al*. Expression of autophagy-related proteins Beclin-1 and LC3A and proliferation marker Ki-67 in calculous and acalculous human gallbladder epithelium. *Hippokratia* 2019; **23:** 64–69.
18. Desai N, Neyaz A, Szabolcs A, *et al*. Temporal and spatial heterogeneity of host response to SARS-CoV-2 pulmonary infection. *Nat Commun* 2020; **11:** 6319.
19. Shahin NN, Abd-Elwahab GT, Tawfiq AA, *et al*. Potential role of aryl hydrocarbon receptor signaling in childhood obesity. *Biochim Biophys Acta Mol Cell Biol Lipids* 2020; **1865:** 158714.
20. Burris HH, Baccarelli AA, Byun HM, *et al*. Offspring DNA methylation of the aryl-hydrocarbon receptor repressor gene is associated with maternal BMI, gestational age, and birth weight. *Epigenetics* 2015; **10:** 913–921.
21. Hascitha J, Priya R, Jayavelu S, *et al*. Analysis of kynurenine/tryptophan ratio and expression of IDO1 and 2 mRNA in tumour tissue of cervical cancer patients. *Clin Biochem* 2016; **49:** 919–924.
22. Théate I, van Baren N, Pilotte L, *et al*. Extensive profiling of the expression of the indoleamine 2,3-dioxygenase 1 protein in normal and tumoral human tissues. *Cancer Immunol Res* 2015; **3:** 161–172.
23. Anti-L-kynurenine. [Accessed 14 July 2021]. Available from: https://www.immusmol.com/l-kynurenine-polyclonal-antibody-rabbit-pab-validated-ihc-if-icc.html
24. Anti-quinolinic acid. [Accessed 14 July 2021]. Available from: https://www.immusmol.com/quinolinic-acid-polyclonal-antibody-rabbit-pab-ihc-icc-if-validated.html
25. Anti-3-hydroxy anthranilic acid. [Accessed 14 July 2021]. Available from: https://www.immusmol.com/3-hydroxyanthranilic-acid-antibody-ihc-mouse-monoclonal-ab.html
26. Wakx A, Nedder M, Tomkiewicz-Raulet C, *et al*. Expression, localization, and activity of the aryl hydrocarbon receptor in the human placenta. *Int J Mol Sci* 2018; **19:** 3762.
27. Anti-CD68. [Accessed 14 July 2021]. Available from: https://www.agilent.com/en/product/immunohistochemistry/antibodies-controls/primary-antibodies/cd68-(concentrate)-76550
28. Anti-CD3. [Accessed 14 July 2021]. Available from: https://www.thermofisher.com/order/genome-database/dataSheetPdf?producttype=antibody&productsubtype=antibody_primary&productId=MA1-90582&version=156
29. Walls AF, Bennett AR, McBride HM, *et al*. Production and characterization of monoclonal antibodies specific for human mast cell tryptase. *Clin Exp Allergy* 1990; **20:** 581–589.
30. Norton AJ, Isaacson PG. Monoclonal antibody L26: an antibody that is reactive with normal and neoplastic B lymphocytes in routinely fixed and paraffin wax embedded tissues. *J Clin Pathol* 1987; **40:** 1405–1412.
31. Anti-S100. [Accessed 14 July 2021]. Available from: https://www.agilent.com/en/product/immunohistochemistry/antibodies-controls/primary-antibodies/s100-(autostainer-autostainer-plus)-76425
32. Anti-cleaved caspase 3. [Accessed 14 July 2021]. Available from: https://www.cellsignal.com/products/primary-antibodies/cleaved-caspase-3-asp175-antibody/9661
33. Anti-LC3b. [Accessed 14 July 2021]. Available from: https://www.cellsignal.com/products/primary-antibodies/lc3b-antibody/2775
34. Anti-Ki67. [Accessed 14 July 2021]. Available from: https://www.abcam.com/ki67-antibody-sp6-ab16667.html
35. Anti-MPO. [Accessed 14 July 2021]. Available from: https://www.agilent.com/en/product/immunohistochemistry/antibodies-controls/primary-antibodies/myeloperoxidase-(dako-omnis)-76205

References 21–35 are cited only in the supplementary material.

SUPPLEMENTARY MATERIAL ONLINE

Supplementary materials and methods

Figure S1. Outcompeting IDO-2 immunohistochemical stain with recombinant hIDO-2 in brain tissue sections from a COVID-19 patient

Figure S2. IDO-2 and 3OH-AA stain of lung tissue from non-COVID-19 patients

Figure S3. IDO-1 and IDO-2 stain of autopsy heart, skeletal muscle, liver, and brain from COVID-19 patients

Figure S4. IDO-2 stain of tissue macrophages (CD68), lymphocytes (CD3), neutrophils (MPO), dendritic cells (S100), mast cells (tryptase), and B lymphocytes (CD20)

Figure S5. IDO-2 stain in brain structures

Table S1. List of Amsterdam UMC COVID-19 Biobank Investigators

Table S2. Demographics of the patients studied using immunohistochemistry

Table S3. Overview of the used antibodies, procedures, and relevant references